UDC 544.77.051+544.172.2+661.682

OPTICAL PROPERTIES AND XPS-CHARACTERIZATION OF Ag/Au BIMETALLIC NANOPARTICLES IN POROUS SOL-GEL SILICA FILMS

A.M. Eremenko,[1,*] N.P. Smirnova,[1] H.R.Yashan,[1] E. Ozkaraoglu,[2] G. Ertas,[2] S. Suzer[2,]

[1] *Chuiko Institute of Surface Chemistry of National Academy of Sciences of Ukraine, 17 General Naumov Street, Kiev 03164, Ukraine*
[2]*Department of Chemistry, Bilkent University, Ankara 06800, Turkey*

Ag/Au bimetallic nanoparticles (BMNP) in porous sol-gel silica films on glass substrates were obtained via hydrolysis of tetraethylorthosilicate (TEOS) in presence of template agent Pluronic P123 and definite amounts of $AgNO_3$ and $HAuCl_4$ by dip-coating procedure followed by a UV-irradiation and thermal treatment. UV-vis spectroscopy was employed to follow the changes in the position and intensity of the surface plasmon resonance band of the resulting BMNP, SEM was employed for morphology investigation. X-ray photoelectron spectroscopy (XPS) was used to determine the chemical states of Au and Ag as well as the surface composition of the resultant films. By utilizing the charging characteristics of the films prepared on a silicon wafer, via application of an external voltage bias, it was found that the Au and Ag nanoparticles are retained within the silica matrix and demonstrate similar charging behavior. Depending on the coating sequences of glass substrates by the silica sol precursors (Au/SiO_2 or Ag/SiO_2), resultant BMNP within silica film have alloy (Au/SiO_2-Ag/SiO_2) or core-shell (Ag/SiO_2-Au/SiO_2) structure.

INTRODUCTION

Silica based materials with embedded nanosized metallic clusters recently have gained a lot of attention due to their catalytic, sensing, non-linear optical properties and the possibility of high-density data storage [1–4]. Insulating silica matrix protects the nanoparticles from the undesirable transformations in outer oxidative medium and under aggressive physical treatments, and intense external fields which are often indispensable in nanodevices' running cycles. Recently, Xiao et al. [5] reported about the possibility of creation of nanobiodevices based on the supported gold nanoparticles. However, it was noted that for certain purposes the application of mixed silver-gold alloy nanoparticles should be more effective than the nanocomposites containing only the corresponding monometallic particles. For instance bimetallic nanostructures could be applied to trace molecules detection as they exhibit much higher sensitivity in SERS analysis [6–8], they also show enhanced catalytic activities in the reactions of *p*-nitrophenol reduction [9], and let it possible to create the polyfunctional switchable biosensors creation [10–11]. In the most common techniques, metal nanoparticles are added to a porous material during gelation, via photoreduction or thermal treatment [12–13]. Sol-gel route is a relatively new method to fabricate thin films on a different type of substrates. This method has been employed to synthesize Ag and Au nanoparticles in SiO_2. Combination of photoreduction and calcination techniques to obtain metal particles from their salts should be effective to produce noble metal NPs within silica composites. Preparation of Ag/Au BMNP from metal salts via simultaneous co-reduction with sodium citrate in laponite suspension [14] or in silica aerogel with formaldehyde [4] results in alloy formation. The authors noted highly inhomogeneous aqua-gel formation, with a low metal concentration in the center, and a high metal concentration at the periphery of the sample what was related to the speed of the reduction process. Successive reduction is generally used to prepare core-shell structures in solutions [15], where the authors reported seed mediated formation of Ag/Au BMNP by UV irradiation where less noble metal formed shell on the preformed NPs of more noble metal, namely synthesis of Ag/Au core-shell NPs in the presence of TX-100.

* Corresponding author *annaerem@ukr.net*

In another work [16], Au NPs coated with silica and deposition of silver on silica was reported. Their TEM images demonstrated the concentric geometry of the particles. A new approach to the synthesis of Ag/Au alloy NPs within silica film consequent deposition of two successive overlapping individual layers of Ag- and Au-doped silica sols respectively on glass substrates followed by the UV irradiation and thermal treatment was proposed in [17] where the authors used TEOS, 3-(glycidoxypropyl) trimethoxysilane, (GLYMO), butanol, methanol, HCl, and aluminium acetylacetonate to maintain two-layers composites. Early we synthesized Ag/Au alloy and core-shell nanoparticles in solutions and within mesoporous silica films by photochemical reduction and/or thermal treatment of the coating [18, 19]. In this work we used the approach proposed in [17] to form "two-layers" porous film by successive introduction of corresponding ions into silica layers, meanwhile the synthesis conditions were essentially changed and simplifyed: porous silica sol-gel films were obtained via template synthesis using amphiphilic triblock copolymer Pluronic P_{123} which acted as templating agent and TEOS as a silica source. P123 can act also as reducing agent of the gold and silver ions in aqueous solutions [20–22]. UV as well as thermal treatment has been employed to treat silica sol with corresponding ions. XPS was used to determine the chemical composition of the resultant sintered films as well as to obtain structure and proximity information about the resultant bimetallic nanoparticles by application of a modification dubbed as the charge-contrast XPS developed recently [23–28].

EXPERIMENTAL

The following chemicals: $AgNO_3$, $HAuCl_4$, tetraethoxysilane 98% (TEOS) (Aldrich) and triblock copolymer Pluronic P_{123}, (BASF) $(PEO)_{19}(PPO)_{69}(PEO)_{19}$, M.W 5400 were used as received. Noble metal nanoparticles containing films were produced using the following procedure. Firstly, 16.2 ml ethanolic sol containing 2.23 ml of TEOS, 1.6 ml 0.10 M nitric acid and 2.0 ml of water has been prepared. After 24 hours of acidic hydrolysis of the TEOS solution, Pluronic 123 in ethanol was added. The resulting molar ratio in starting precursor sol was $1TEOS:1.5H_2O:0.16\ HNO_3:39EtOH:0.011P_{123}$. The resulting films on glass and silicon wafer substrates were generated by two sequential dip-coating procedures for realizing two layers coating. The first layer contained Ag^+ ions and the second one contained $AuCl_4^-$ ions (Film 1) or the first layer contained $AuCl_4^-$ ions and the second one contained Ag^+ ions (Film 2). After low temperature (60 ^oC) drying for several minutes, the samples were irradiated under UV-light for 90 minutes. A 1000-W high-pressure mercury lamp supplied with the standard chemical light filter ($CoSO_4 \times 7H_2O$ – 8.4 g/100 ml H_2O) was used as an irradiation source for 253.7 nm light. Incident photon intensity (as determined by a tris(oxalato)ferrate(III)actinometer) at 253.7 nm was of $2*10^{17}$ quant$\cdot cm^{-2}\cdot s^{-1}$. Contents of silver and gold ions were 5% at. Ag and 5% at. Au considering the amount of TEOS as being 100%. Then the film was heat-treated at 500°C for 3 hours. The procedure is schematically described in Scheme 1. Thus, it is clear that the structures of silica matrices doped with metal NPs obtained in [17] and in this work are different.

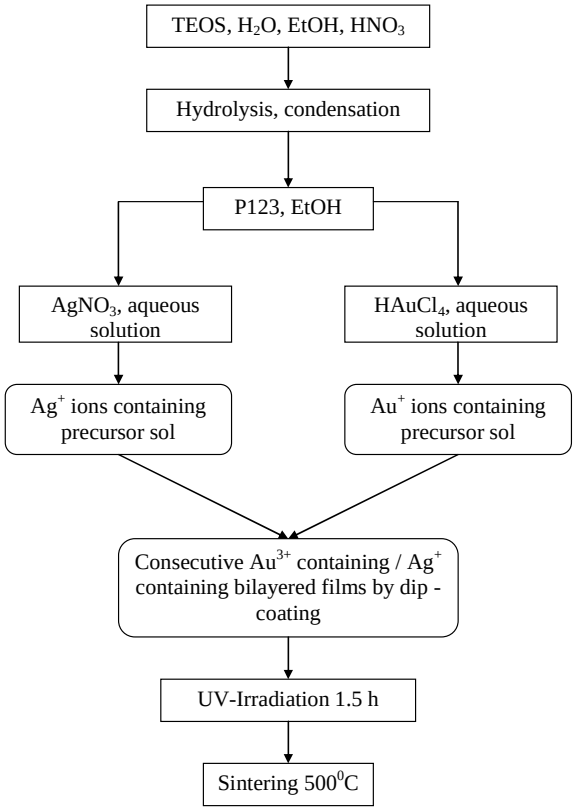

Scheme I. Synthesis flow diagram.

A Lambda Bio-40 UV-Vis spectrometer was used for optical characterization of the films prepared on glass slides, and a Leo 1530 Scan-

ning Electron Microscope was used for the SEM images of the films prepared on silicon wafers. XPS characterization of samples were carried out using a Kratos ES300 electron spectrometer with MgKα X-rays (unmonochromized, 1253.6 eV). In the standard geometry the sample accepts X-rays at 45° and emitted photoelectrons at 90° with respect to its surface plane are analyzed. Films prepared on silicon wafer substrates were electrically connected to the sample holder, which was grounded or externally biased with a d.c. power supply. A nearby filament provides low energy electrons for charging/discharging of the sample under investigation.

RESULTS AND DISCUSSION

Optical and Structural Characterization. It is well-known that triblock-copolymers, along with template agents to form porous silica films, act as the effective reducing agents and stabilizers of noble metal nanoparticles [29] due to polyethylene oxide groups

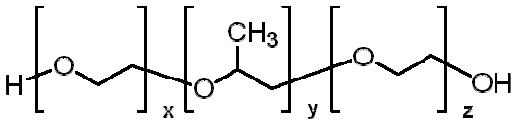

Formation of NPs includes the next stages:

1) Adsorption of Ag^+ (or $AuCl_4^-$) on the hydrophilic groups of triblock-copolymer.
2) Reduction of metal ions under UV-irradiation.
3) Adsorption of the atoms and clusters of the metal NPs on the surface of hydrophobic PO-groups.
4) Metal NPs growth under thermal treatment of the film.

Thus P_{123}' role in the synthesis is dual, notably the porous structure of silica formation and reduction of metal ions to the metal NPs, which are localized on the surface and within silica pores. It is clear in the SEM images.

After deposition of the first Ag-salt containing silica layer and drying, then the Au-salt containing silica layer, drying and UV-irradiation (film 1), the main band in the optical spectra is located at 587 nm with the shoulder at 400 nm (Fig. 1 *a*). In this case we suggest the formation of core Ag – shell Au structure within silica film.

The SEM images of the sintered film 1 are shown in the Fig. 1 *b*. with BMNP located in pores. BMNP with dark core and light shell have average radii of app. 20 nm. Similar conclusion on the structure of BMNP particles has been done in [30].

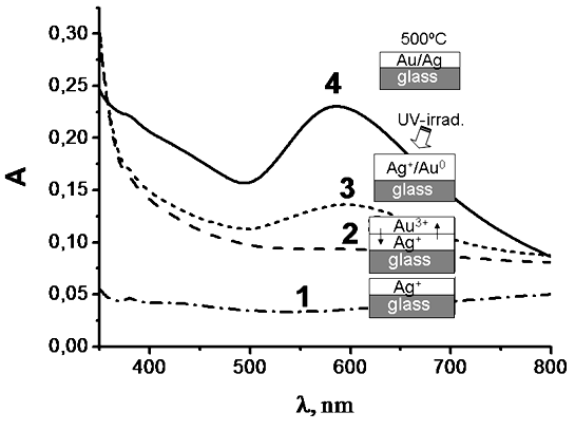

Fig. 1. ***a*** Absorption spectra of film 1 after deposition of the first Ag containing layer and drying – 1; - after deposition of the second Au containing layer and drying–2; after irradiation – 3; after sintering – 4.

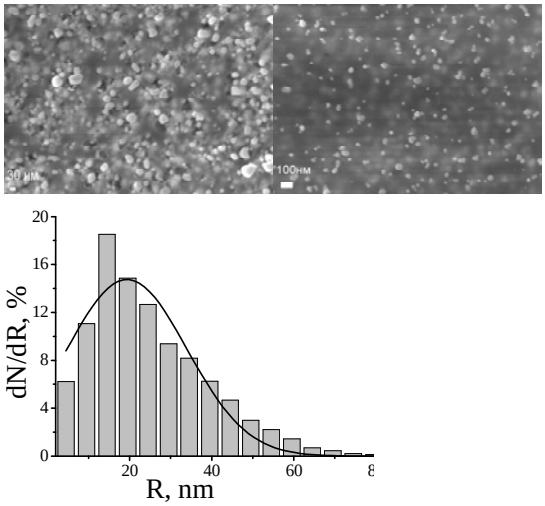

Fig. 1. ***b***. SEM images and size distribution of nanoparticles in film 1 after treatment.

Optical spectra of the film 2 on the glass slide at different preparation steps are shown in the Fig. 2. It is seen that after deposition of the first Au-salt containing silica layer and drying no plasmon maximum occurred (sp.1). After depositing the second silica layer containing the Ag salt, and drying, the film shows a weak Au surface plasmon resonance (SPR) band, with a diffuse maximum at app. 554 nm belonging to the Au seeds, formed during the treatment [31–36]. Presence of small amount of Ag^+ ions from the top layer accelerates the nucleation of Au nanoparticles in accordance with [30].

After irradiation, the SPR band of gold at 546 nm becomes much more intense, also because of the inner photoreaction in $AuCl_4^-$, which forms the charge transfer excited complexes, where gold can abstract electrons from chlorine ions [36], and also some residual amount of alcohol may contribute to the photoreduction process [37–38]. After thermal treatment at 500°C the SPR band maximum of the film is observed to move to 500 nm. Such a behavior should indicate the formation of random alloy nanoparticles. The Au/Ag alloy formation is supported by the fact that the optical absorption spectrum shows only one plasmon peak which is also blue-shifted from the region of gold nanoparticles absorption. The absorption band position is dependent mainly on the surface chemical composition, namely Au:Ag ratio. The maximum absorption wavelength with the 50% gold mole fraction deviated from a linear relationship with maximum corresponding to the alloy composition (in solution, with the Au/Ag ratio 1:1, the position of the alloy absorption maximum should be at around 470–480 nm). One can suggest that after thermal treatment of Au-Ag/SiO_2 at 500^0 C, the Au-Ag composition is different from that in the solution or bulk. In our case when Au-Ag clusters are constrained within silica film we suggest that the alloy is not regular, with Au atoms domination in the particle composition.

Moreover, [39] noted for the Au-Ag clusters, although the surfaces were predicted to be Ag rich, the ionic contribution was observed to drive some of the Au atoms to the surface as it favored an Ag-Au mixture. A physical mixture of synthesized individual Au and Ag colloids demonstrates two plasmon peaks corresponding to the monometallic NPs. The overall spectral changes are consistent with the formation of Ag-Au alloys enriched with Au atoms.

The SEM images of the sintered film 2 are shown in Fig. 2 ***b***. The porous nature of the sol-gel derived silica matrix is apparent from the less magnified SEM image, and the presence of metal nanoparticles distributed throughout the silica-gel matrix is better seen in the more magnified image. Note that small metal nanoparticles with sizes of 3 nm or less would go completely undetected both with respect to their optical signature, since they would not have enhanced SPR signals, and also with respect to their SEM images.

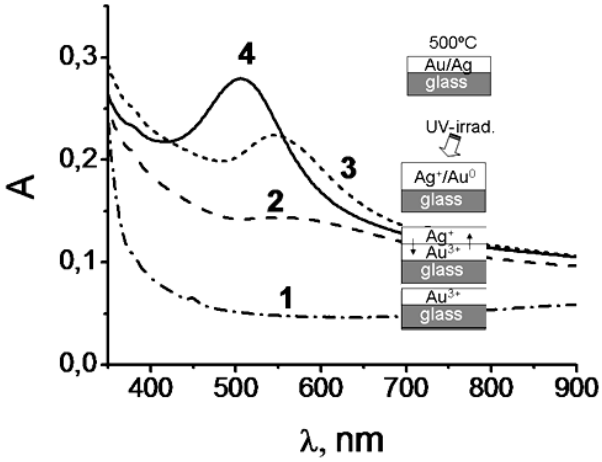

Fig. 2. *a.* Absorption spectra of film 2 after deposition of the first Au containing layer and drying – 1; 2 – after deposition of the second Ag containing layer and drying; 3 – after irradiation; 4 – after sintering.

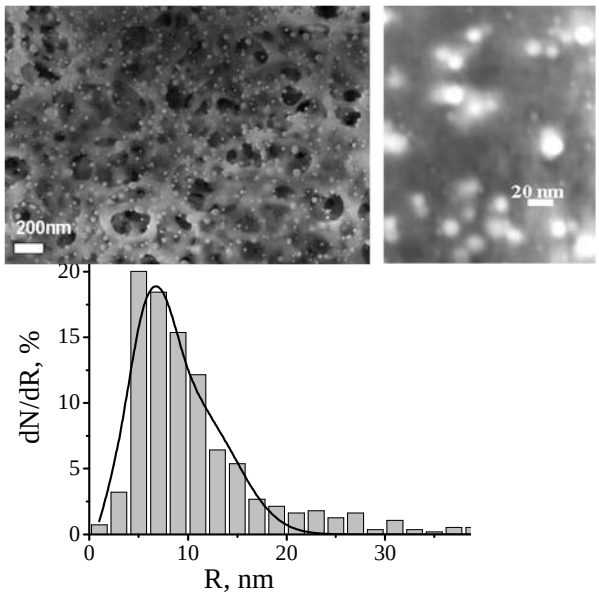

Fig. 2 *b*. SEM images and size distribution of nanoparticles in film 2 after treatment.

XPS Analysis. Although XPS is a powerful analytical spectroscopic tool with elemental and chemical specificity, it is a surface sensitive technique and has a probe depth of only 12 nm. The results of XPS analysis given as an example for the film 2 are given in Table 1. Peaks belonging to oxygen (O1s) and silicon (Si 2p and 2s) are the prominent features and the Ag3d and Au4f peaks are quite weak. When referenced to the tabulated value of the Si2p of the oxide (Si^{4+}) at 103.2 eV, the measured binding energies of the Au4f and Ag3d peaks are determined as 84.3 and 368.4 v respectively.

Table 1. Atomic ratios determined from XPS

Ag/Au/SiO_2 film (on silicon)- Film1 Electron Take-Off Angle = 90°	1.0	2.2	0.005	0.006
Au/Ag/SiO_2 film (on silicon)-Film2	**Si**	**O**	**Au**	**Ag**
Electron Take-Off Angle = 90°	1.0	2.2*	0.013	0.023
= 30°**	1.0	-	0.012	0.017

*Slightly higher than 2 for O, probably means that the sol-gel derived oxide layer contains extra water or –OH species.
**Measurements at 30 refers to more surface sensitivity, i.e. probed only the top 6 nm.

These values are slightly higher than the corresponding zero valence states of both metals (Au^0, Ag^0), but lower than those corresponding to their ionic states [40], and their atomic ratios are 2.3 and 1.3 at. %, with respect to Si. Firstly, the presence of more Ag than Au must be related with the order in which these salts were introduced into the film (gold as the first layer and silver as the second and the outermost one). Secondly, these ratios decrease to 1.7 and 1.2 at. % when the data is recorded at the more surface sensitive electron take-off angle of 30°. Both of these observations are consistent with complete reduction and embedding of the nanoparticles into the resulting silica-gel matrix.

The Si2p region is complicated and consists of features belonging to both unoxidized (Si^0) and oxidized (Si^{4+}) forms of silicon. The presence of Si^0 is not very surprising due to the porous nature of the film, and also probably due to the incomplete coverage of the silicon substrate with the sintered silica-gel film. However, this introduces another problem, because we must also take into account the native oxide layer (ca. 2 nm thick), if correct stoichiometry of the silica-gel matrix is to be determined, since the Si2p peak of the native oxide and that of the sol-gel matrix overlap completely. At this point we turn to our powerful charge-contrast methodology that we have developed in recent years [23–28].

For poorly conducting samples, XPS encounters a series of problem with charging, since photoelectrons leaving the sample under investigation result in a positively charged surface. This obstacle has long been overcome by various neutralization techniques developed [37]. However, this nuisance can also be converted into a useful tool for extracting additional information, since the extent of charging can be controlled by application of an external bias to the sample, while recording XPS data. Furthermore, this simple experimental trick enables us to extract additional analytical information about the distribution of various elements in layered or composite structures, as in the present case, where by purposely charging the sample, we are able to resolve the overlapping components of the peaks belonging to the sol-gel matrix from those of the native oxide [23–28].

This is best explained by application of our method to a sample of silicon wafer containing a thin thermal oxide of ca. 2 nm thickness. The Si^{4+} and the Si^0 peaks of the Si2p region belonging to the oxide and to the substrate, respectively, can easily be distinguished due to the large chemical shift between them. However, the measured binding energy difference can easily be changed by application of an external voltage bias to the sample, due to charging, as shown in Figure 3. Under -10 V bias, neutralizing electrons from the filament are repelled completely away from the sample which causes positive charging in the oxide layer, hence the binding energy difference increases. Under +10 V, the electrons are drawn into the sample to neutralize the positive charging. If, the current of the filament increases, the oxide layer becomes negatively charged and the shift becomes smaller and smaller to the extent that the oxide peaks starts exhibiting a negative chemical shift. Another characteristic of the negative charging is the accompanying broadening of the peaks. Obviously, any other element present within the oxide layer would also exhibit a parallel shifting and/or broadening behavior, what is a very important analytical tool in terms of yielding proximity and/or lateral information about the samples analyzed [23–28].

A similar analysis of the sample under consideration for the region of the Si2p and Au4f, is given in Fig. 4. a. For simplicity, we only show spectra corresponding to the uncharged and progressively more negatively charged situations.

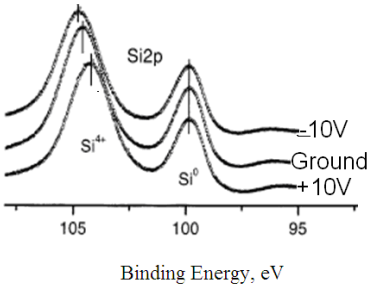

Fig. 3. Si2p region of the XPS spectrum of a silicon wafer sample containing ca. 5 nm thermal oxide layer. As the oxide layer becomes progressively more negatively charged the peak starts exhibiting a negative binding energy shift and becomes broader.

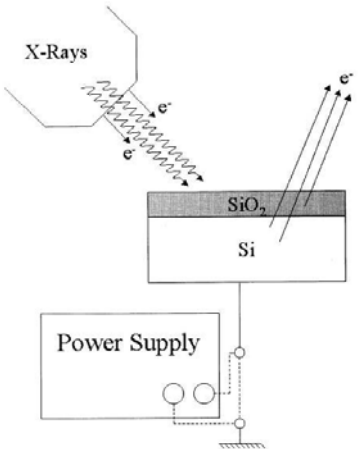

There are only two Si2p peaks in the spectrum of uncharged sample, corresponding to the substrate (Si^0) and a composite peak of the oxide layers ($Si^{\delta+}$). As the sample becomes negatively charged, the oxide peak is split into 2 peaks, one of which does not shift, but the other shifts progressively to lower energies and becomes broader. The nonshifting peak belongs to the thin native oxide layer, and the shifting one can now be assigned to the oxide layer prepared by the sol-gel technique. Similar to the Si-oxide peak, the O1s peak splits into two components corresponding to the native and sol-gel oxide layers, respectively, as shown in Fig. 4 ***b***. Interestingly, the Au4f and the Ag3d, exhibit exactly the same shifting behavior. This means that all of Au and Ag nanoparticles are retained within the sol-gel matrix after sintering. Secondly, since we can separate the peaks of the native oxide and the sol-gel layers, a more accurate stoichiometry can be calculated (as given in Table 1). Thirdly, as was pointed out in the optical characterization part, the alloy nature of the nanoparticles is also brought up in our charge-contrast XPS analysis, since the shifts of the Au4f and the Ag3d are exactly the same.

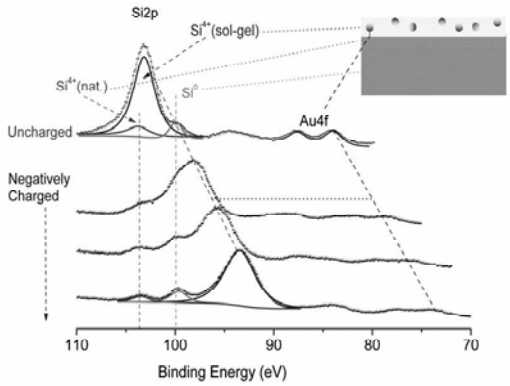

Fig. 4 *a*. Si2p-Au4f region of the XPS spectrum of $AuAg/SiO_2$, under uncharged, and as progressively negatively charged states. Note that the Au4f peak shifts parallel to the silicon oxide layer prepared by sol-gel route.

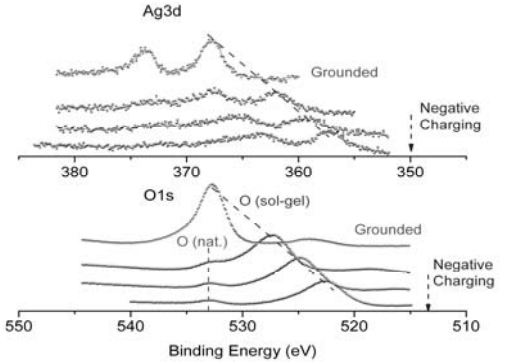

Fig. 4 *b*. O1s (bottom) and Ag3d (top) regions of the XPS spectrum, under uncharged, and as progressively negatively charged states. Note that the Ag3d peak shifts parallel to the silicon oxide layer prepared by sol-gel route. The O1s peak splits into two corresponding to the native and the sol-gel oxide layers.

Independently on the precursor order in the two-layer coating, upper layer of the final Film2 is enriched with Ag particles (Table 1). We have to take into account that the penetration depth during the XPS analysis is of 10-12 nm, so the calculated data of atomic ratios determined from XPS (Table 1) represent this thin layer. In case of Film 2 with alloy morphology of BMNP, the Au:Ag ratio calculated from XPS data is 1:1,8. When core-shell BMNP in case of Film 1, this ratio is 1:1,2. We suppose that part of Ag NPs is uncoupled with Au and diffused to the upper layer of composites. Thus, template synthesis using TEOS as a silica film source, triblock copolymer, and successive coating of Au- and Ag-precursors results in thin and highly porous silica films with embedded and protected bimetallic nanoparticles with different morphology.

CONCLUSIONS

In this work, we investigated the optical properties and morphology of Au/Ag bimetallic nanoparticles within transparent porous sol-gel silica film prepared by sequential dip-coating of Au - and Ag - silica precursors using the combination of UV-irradiation and thermal treatment of the film as reduction processes. The films were investigated by UV-vis, SEM and XPS methods. Optical spectra of film 1 did not demonstrate significant shifts during the formation of BMNP within silica matrix. The SPR band is typical of the core-shell structure. Optical spectra of film 2 in each step of the preparation route demonstrate the blue shift on the stages of BMNP formation and enclose the SPR band typical of the alloy structures. SEM images gave evidences on the formation of small particles embedded under the surface and walls of porous silica film. By utilizing the X-ray photoelectron spectroscopy and charging characteristics of the films prepared on a silicon wafer, via application of an external voltage bias, it has been found that the Au and Ag nanoparticles are retained within the silica matrix, and demonstrate similar charging behavior. Taking into account the penetration depth during the XPS analysis, the calculated data of atomic ratios determined from XPS (Table 1) do not represent exactly the bimetallic composition of outer layer. Simple method of the sol-gel template synthesis using TEOS as a silica film source and successive coating of Au- and Ag- precursors results in thin and highly porous silica films with embedded and protected bimetallic nanoparticles with alloy or core-shell structure.

Acknowledgement. We thank Dr. Christopher Tabor of Georgia Institute of Technology for the help in SEM measurements. This work has been supported by the joint TUBITAK-NASU, the Scientific and Technological Research Council of Turkey, and the National Academy of Sciences of Ukraine, through the Joint Research Project No: 106T713.

REFERENCES

1. *Gonella F., Mazzoldi P.* Metal nanocluster composite glasses // Handbook in Nanostructured materials and nanotechnology. – San Diego: Acad. Press, 2000. – V. 4. – P. 81–158.
2. *Choudhary T.V., Sivadinarayana C., Chusuei C.C. et al.* CO oxidation on supported nano-Au catalysts synthesized from a $[Au_6(PPh_3)_6](BF_4)_2$ complex // J. Catal. – 2002. – V. 207. – P. 247–255.
3. *Wallace J.M., Rice J.K., Pietron J.J. et al.* Silica nanoarchitectures incorporating self-organized protein superstructures with gas-phase bioactivity // Nano lett. – 2003. – V. 3. – P. 1463–1467.
4. *Hund J.F., Bertino M.F., Zhang G. et al.* Synthesis of homogeneous alloy metal nanoparticles in silica aerogels // J. Non-Cryst. Solids. – 2004. – V. 350. – P. 9–13.
5. *Xiao Y. , Patolsky F. , Katz E. et al.* "Plugging into enzymes": nanowiring of redox enzymes by a gold nanoparticle // Science. – 2003. – V. 299. – P. 1877–1881.
6. *Liu Y.C. , Yu C.C., Hsu T.C.* Trace molecules detectable by surface-enhanced Raman scattering based on newly developed Ag and Au nanoparticles-containing substrates // Electrochem. Commun. – 2007. – V. 9. – P. 639–644.
7. *Xu S. , Zhao B. , Xu W. et al.* Preparation of Au–Ag core-shell nanoparticles and application of bimetallic sandwich in surface-enhanced Raman scattering (SERS) // Colloids Surf., A. – 2005. – V. 257–258. – P. 313–317.
8. *Liu Y.C., Yang K.H., Yang S.J.* Sonoelectrochemical synthesis of spike-like gold–silver alloy nanoparticles from bulk substrates and the application on surface-enhanced Raman scattering // Anal. Chim. Acta. – 2006. – V. 572. – P. 290–294.
9. *Endo T., Yoshimura T., Esumi K.* Synthesis and catalytic activity of gold–silver binary

nanoparticles stabilized by PAMAM dendrimer // J. Colloid Interface Sci. – 2005. – V. 286. – P. 602–609.
10. *Ren X., Meng X. , Tang F.* Preparation of Ag–Au nanoparticle and its application to glucose biosensor // Sens. Actuators, B. – 2005. – V. 110. – P. 358–363.
11. *Cao Y.C., Jin R., Nam J.M. et al.* Raman dye-labeled nanoparticle probes for proteins // J. Am. Chem. Soc. – 2003. – V. 125. – P. 14676–14677.
12. *Hund J.F., Bertino M.F., Zhang G. et al.* Formation and entrapment of noble metal clusters in silica aerogel monoliths by γ-radiolysis // J. Phys. Chem. B. – 2003. – V. 107. – P. 465–469.
13. *Morris C.A., Anderson M.L., Stroud R.M. et al.* Silica sol as a nanoglue: flexible synthesis of composite aerogels //Science. – 1999. – V. 284. – P. 622–624.
14. *Aihira N., Torigoe K., Esumi K. et al.* Preparation and characterization of gold and silver nanoparticles in layered laponite suspensions // Langmuir. – 1998. – V. 14. – P. 4945–4949.
15. *Malik K., Mandal M., Pradhan N. et al.* Seed mediated formation of bimetallic nanoparticles by UV Irradiation: a photochemical approach for the preparation of "core−shell" type structures // Nano lett. – 2001. – V. 1. – P. 319–322.
16. *Schierhorn M., Liz-Marzan M.* Synthesis of bimetallic colloids with tailored intermetallic separation // Nano lett. – 2002. – V. 2. – P. 13–16.
17. Pal S., De G. A new approach for the synthesis of Au-Ag alloy nanoparticle incorporated SiO_2 films // Chem. Mater. – 2005. – V. 17. – P. 6161–6166.
18. *Yashan H., Eremenko A., Smirnova N. et al.* Optical spectra and morphology of photochemically produced Ag/Au bimetallic clusters // Sol-Gel Methods for Materials Processing (ARW NATO) / Eds. P.Innocenzi, Yu.Zub, V.Kessler. – Springer: – 2008. – P. 473–480.
19. *Yashan G.R. , Eremenko A.M. , Smirnova N.P. et al.* Morphology and optical properties of thin silica films containing bimetallic Ag/Au nanoparticles // Theoret. Experim. Chemistry. – 2008. – V. 44, N 6. – P. 356–361.
20. Sakai T., Alexandridis P. Mechanism of gold metal ion reduction, nanoparticle growth and size control in aqueous amphiphilic block copolymer solutions at ambient conditions // J. Phys. Chem. B. – 2005. – V. 109. – P. 7766–7777.
21. *Chen D-H., Huang Y-W.* Spontaneous formation of Ag nanoparticles in dimethylacetamide solution of poly(ethylene glycol) // J. Colloid Interface Sci. – 2002. – V. 255. – P. 299–302.
22. *Longenberger L., Mills G.* Formation of metal particles in aqueous solutions by reactions of metal complexes with polymers // J. Phys. Chem. – 1995. – V. 99. – P. 475–478.
23. *Suzer S.* Differential charging in x-ray photoelectron spectroscopy: a nuisance or a useful tool? // Anal. Chem. – 2003. – V. 75. – P. 7026–7029.
24. *Karadas F., Ertas G., Suzer S.* Differential charging in SiO_2/Si system as determined by XPS // J. Phys. Chem. B. – 2004. – V. 108. – P. 1515–1518.
25. *Ertas G., Suzer S.* XPS analysis with external bias: a simple method for probing differential charging // Surf. Interface Anal. – 2004. – V. 36. – P. 619–623.
26. *Demirok U.K., Ertas G., Suzer S.* Time-resolved XPS analysis of the SiO_2/Si system in the millisecond range // J. Phys. Chem. B. – 2004. – V. 108. – P. 5179–5181.
27. *Suzer S., Dana A., Ertas G.* Differentiation of domains in composite surface structures by charge-contrast X-ray photoelectron spectroscopy // Anal. Chem. – 2007. – V. 79. – P. 183–186.
28. *Sezen H., Ertas G., Dana A. et al.* Charging/discharging of thin PS/PMMA films as probed by dynamic X-ray photoelectron spectroscopy // Macromolecules. – 2007. – V. 40. – P. 4109–4112.
29. *Sakai T., Alexandridis P.* Facile preparation of Ag–Au bimetallic nanonetworks // Mater. Lett. – 2006. – V. 60. – P. 1983–1986.
30. *Shankar S. S., Rai A., Ahmad A. et al.* Rapid synthesis of Au, Ag, and bimetallic Au core–Ag shell nanoparticles using Neem (Azadirachta indica) leaf broth // J. Colloid Interface Sci. – 2004. – V. 275. – P. 496–502.
31. *Shibata T., Bunker B.A., Zhang Z. et al.* Size-dependent spontaneous alloying of Au−Ag nanoparticles // JACS. – 2002. – V. 124. – P. 11989–11996.
32. *Link S., El-Sayed M.A. et al.* Spectroscopic determination of the melting energy of a gold nanorod // J. Chem. Phys. – 2001. – V. 114. – P. 2362–2368.
33. *Mohamed M., Izmail K.Z., Link S. et al.* Thermal reshaping of gold nanorods in mi-

celles // J. Phys. Chem. B. – 1998. – V. 102. – P. 9370–9374.
34. *Kim F., Connor S., Song H. et al.* Platonic gold nanocrystals // Angew. Chem. Int. Ed. – 2004. – V. 43. – P. 3673–3677.
35. *Silvert P.-Y., Tekaia-Elhsissen K.* Synthesis of monodisperse submicronic gold particles by the polyol process // Solid State Ionics. – 1995. – V. 82. – P. 53–60.
36. *Henglein A.* Radiolytic preparation of ultrafine colloidal gold particles in aqueous solution: optical spectrum, controlled growth, and some chemical reactions // Langmuir. – 1999. – V. 15. – P. 6738–6744.
37. *Zhu J., Wang Y. , Huang L. et al.* Resonance light scattering characters of core–shell structure of Au–Ag nanoparticles // Phys. Lett. A. – 2004. – V. 323. – P. 455–459.
38. *Schwarz H.A., Dodson R.W.* Reduction potentials of CO_2^- and the alcohol radicals // J. Phys. Chem. – 1989. – V. 93. – P. 409–414.
39. *Ferrando R., Jellinek J., Johnston R.L.* Nanoalloys: from theory to applications of alloy clusters and nanoparticles // Chem. Rev. – 2008. – V. 108. – P. 845–910.
40. *Briggs D., Seah M.P.* Practical surface analysis. Part 1. – 2nd ed. – London: J. Wiley & Sons, 1996. – 533 p.

Received 01.03.2010, accepted 16.03.2010

Оптичні властивості та РФЕС-характеризація біметалічних наночастинок Ag/Au в пористих силікатних золь-гель плівках

Г.М. Єременко, Н.П. Смірнова, Г.Р. Яшан, Е. Оскароглу, Г. Ерташ, Ш. Сюзер

Інститут хімії поверхні ім. О.О. Чуйка Національної академії наук України
вул. Генерала Наумова 17, , Київ 03164, Україна, annaerem@ukr.net
Факультет хімії університету Білкент, Анкара 06800, Туреччина

Біметалічні наночастинки (БМНЧ) Ag/Au, інкорпоровані в пористу золь-гель кремнеземну плівку, були одержані шляхом гідролізу тетраетилортосилікату (ТЕОС) в присутності темплатного агента Pluronic P123 з додаванням $AgNO_3$ і $HAuCl_4$; нанесення плівок на субстрат проводилося методом "dip-coating" з наступним УФ-опроміненням і термообробкою. УФ- видима спектроскопія застосовувалася для реєстрації положення і інтенсивності максимумів поверхневого плазмонного резонансу БМНЧ, а рентгено-фотоелектронна спектроскопія - для визначення хімічного стану Au і Ag та встановлення поверхневого складу плівки. При використанні методики заряджения плівок на кремнієвій підкладинці шляхом накладання зовнішнього електричного потенціалу було встановлено, що наночастинки Au і Ag зв'язані з силікатною матрицею та демонструють однаковий відгук на накладений зовнішній негативний потенціал. В залежності від послідовності нанесення прекурсорів (Ag/SiO_2 або Au/SiO_2) на підкладинку, БМНЧ, які містяться в матриці кремнеземної плівки, формують структуру типу сплав (Au/SiO_2-Ag/SiO_2) або ядро-оболонка(Ag/SiO_2-Au/SiO_2).

Оптические свойства и РФЭС-характеризация биметаллических наночастиц Ag/Au в пористых силикатных золь-гель пленках

А.М. Еременко, Н.П. Смирнова, Г.Р. Яшан, Э. Оскароглу, Г. Эрташ, Ш. Сюзер

Институт химии поверхности им. А.А.Чуйко Национальной академии наук Украины,
ул. Генерала Наумова 17, Киев 03164, Украина, annaerem@ukr.net
Факультет химии университета Билкент, Анкара 06800, Турция

Биметаллические наночастицы (БМНЧ) Ag/Au, инкорпорированные в пористую золь-гель кремнеземную пленку, были получены путем гидролиза тетраэтилортосиликата (ТЭОС) в присутствии темплатного агента Pluronic P123 с добавлением $AgNO_3$ и $HAuCl_4$; нанесение пленок на субстрат производилось методом "dip-coating" с последующим УФ-облучением и термообработкой. УФ-видимая спектроскопия использовалась для регистрации изменений в положении и интенсивности максимумов поглощения полос поверхностного плазмонного резонанса БМНЧ, а рентгено-фотоэлектронная спектроскопия – для определения химического состояния Au и Ag и установления поверхностного состава пленки. С помощью методики заряжения пленок на кремниевой подложке путем наложения внешнего электрического потенциала было установлено, что наночастицы Au и Ag связаны с силикатной матрицей и демонстрируют одинаковый отклик на приложенный внешний негативный потенциал. В зависимости от последовательности нанесения прекурсоров (Ag/SiO_2 или Au/SiO_2) на подложку, БМНЧ в матрице кремнеземной пленки образуют структуру типа сплав (Au/SiO_2-Ag/SiO_2) или ядро-оболочка (Ag/SiO_2-Au/SiO_2).